

Supplementary Information

The swelling mechanism of ethylene-Vinyl acetate polymer in different solvents via molecular dynamics and experimental studies

Rui Luo^c, Jinniu Miao^d, Yihan Zhao^c, Shengbin Chen^c, Yang Yang^c, Qiang Lu^{a,b,c}, Bin Hu^{a,b,c}, Bing Zhang^{a,b,c*} and Ji Liu^{a,b,c*}

^a National Engineering Research Center of New Energy Power Generation, North China Electric Power University, Beijing 102206, People's Republic of China

^b State Key Laboratory of Alternate Electrical Power System with Renewable Energy Sources, North China Electric Power University, Beijing 102206, People's Republic of China

^c School of New Energy, North China Electric Power University, Beijing 102206, People's Republic of China

^d China Petroleum Pipeline Engineering Corporation, Langfang 065000, China

*Bing Zhang (E-mail: mpezb310@gmail.com)

*Ji Liu (E-mail: liujipower@ncepu.edu.cn)

S1. The RMSD data of the EVA aggregate in the three systems.

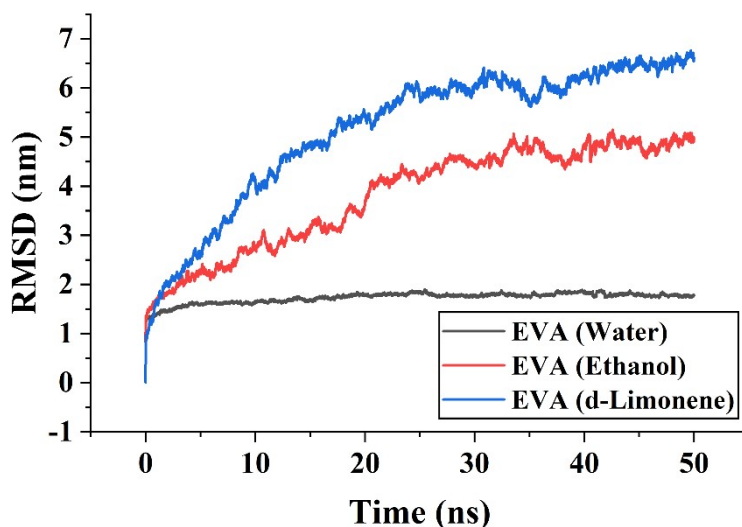


Fig. S1. The RMSD data of the EVA aggregate in the water, ethanol, and d-limonene systems.

As shown in the Fig. S1, the RMSD curve of the EVA aggregate in water quickly stabilized around 1.8 nm after the start of the simulation, indicating that the system rapidly reached equilibrium. In ethanol and d-limonene, the RMSD curves rose rapidly after the start of the simulation, with the upward trend gradually slowing down after 25 ns. The former stabilized within 4.5 - 5 nm after 30 ns, while the latter stabilized within 6 - 7 nm after 40 ns, with both systems reaching equilibrium.

S2. The RMSD data of each EVA chain in the three systems.

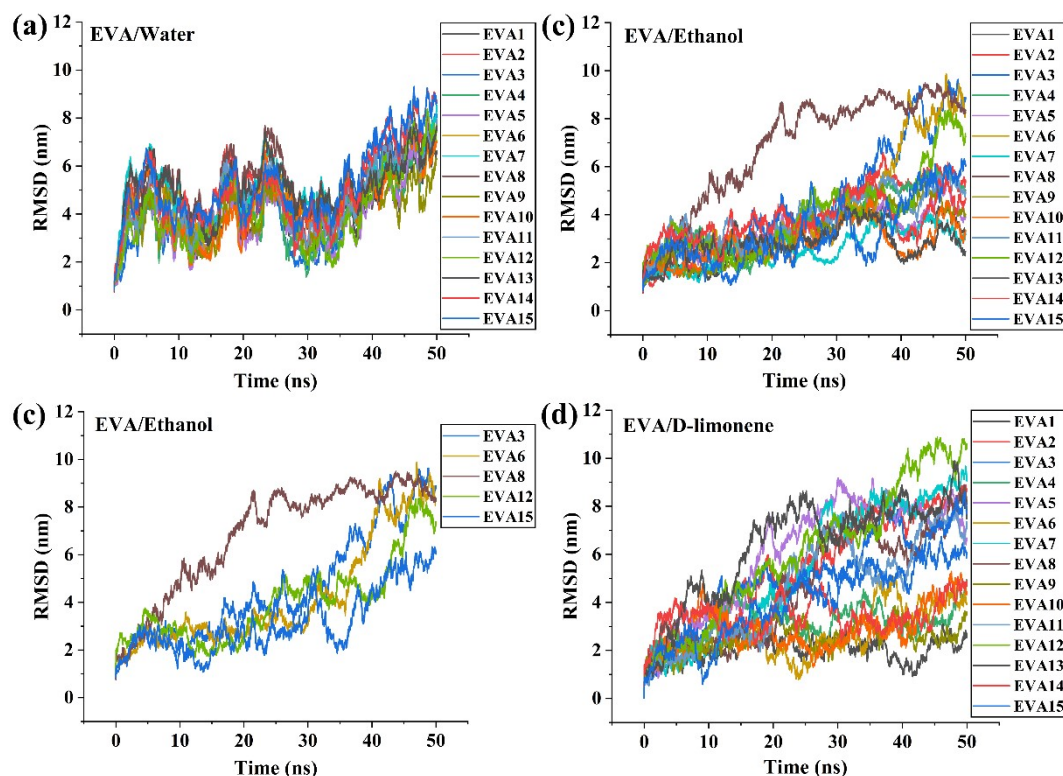


Fig. S2. The RMSD curves of the EVA chains in water (a), ethanol (b) and d-limonene (d), respectively. The RMSD curves of the EVA3, EVA6, EVA8, EVA12, and EVA15 chains in ethanol (c).

In the EVA/water system, the RMSD values of all the EVA chains mainly fluctuate in the range of 2 nm to 8 nm. The fluctuations of all the chains are synchronized, indicating no significant structural change differences has been detected among the chains. In the EVA/ethanol system, the EVA3, 6, 8, 12, and 15 chains exhibit evident RMSD variations. The RMSD curve of EVA3 gradually rises from 2 nm to 9 nm during the 50-ns process. For EVA6, and EVA12, their RMSD values swiftly increase from approximately 4 nm to over 8 nm after 30 ns and that of EVA8 rapidly rises from 2 nm to stabilize at around 9 nm following the start of the simulations. EVA15 firstly experiences an intense fluctuation between 2 - 5 nm and then increases to 6 nm after 35 ns. The other 10 chains show similar trends in the growth of RMSD, whose values gradually increase to, yet stay below, 6 nm. This indicates that the five EVA chains have undergone specific structural changes relative to the other chains. In

the EVA/d-limonene system, the RMSD values change from approximately 1 nm to 11 nm during the 50-ns simulations, and those of nine chains are ultimately greater than 6 nm, which reveals that most of the EVA chains experience significant structural changes and exhibit differences from each other.

S3 The aggregation state changes between d-limonene molecules and EVA chains.

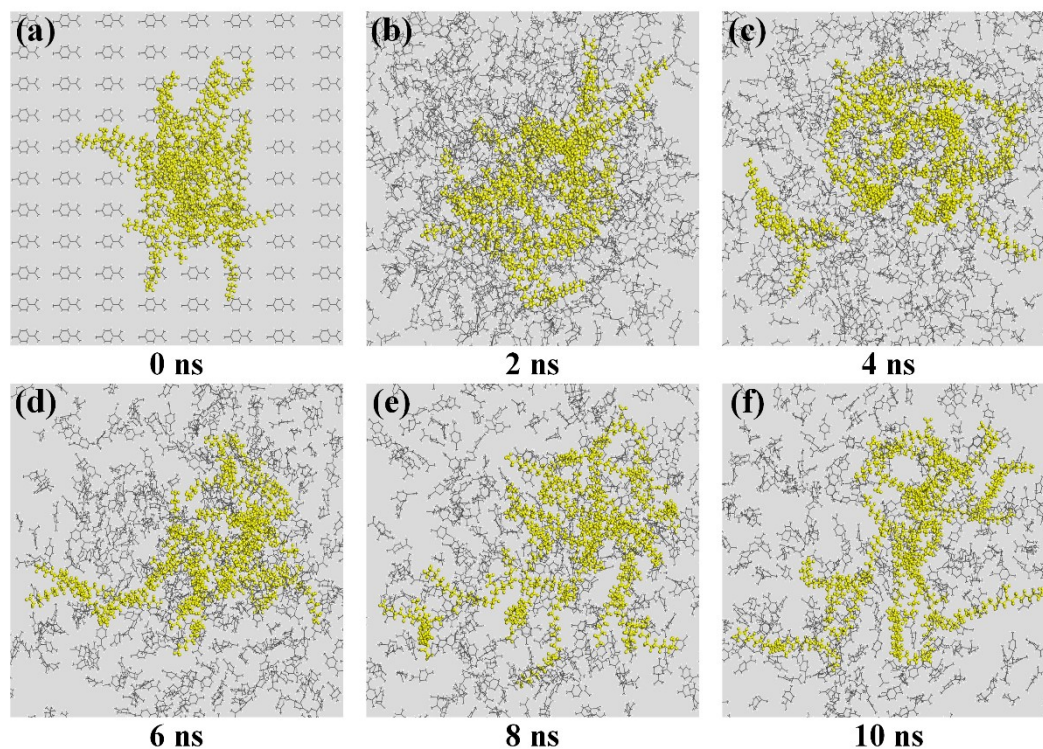


Fig. S3. The aggregation state changes between d-limonene molecules and EVA chains within the first 10 ns.

After the simulation starts, d-limonene molecules rapidly draw close to the EVA polymers as displayed in Fig. S3. By 2 ns, d-limonene molecules have tightly enveloped the EVA chains, and the two are in a tight aggregation state. It can be seen from the subsequent structural changes that d-limonene molecules gradually enter the interior of the EVA aggregate and distribute among the gaps of the chains, leading to a gradual separation of the EVA chains.

S4. The aggregation state changes between ethanol molecules and EVA chains.

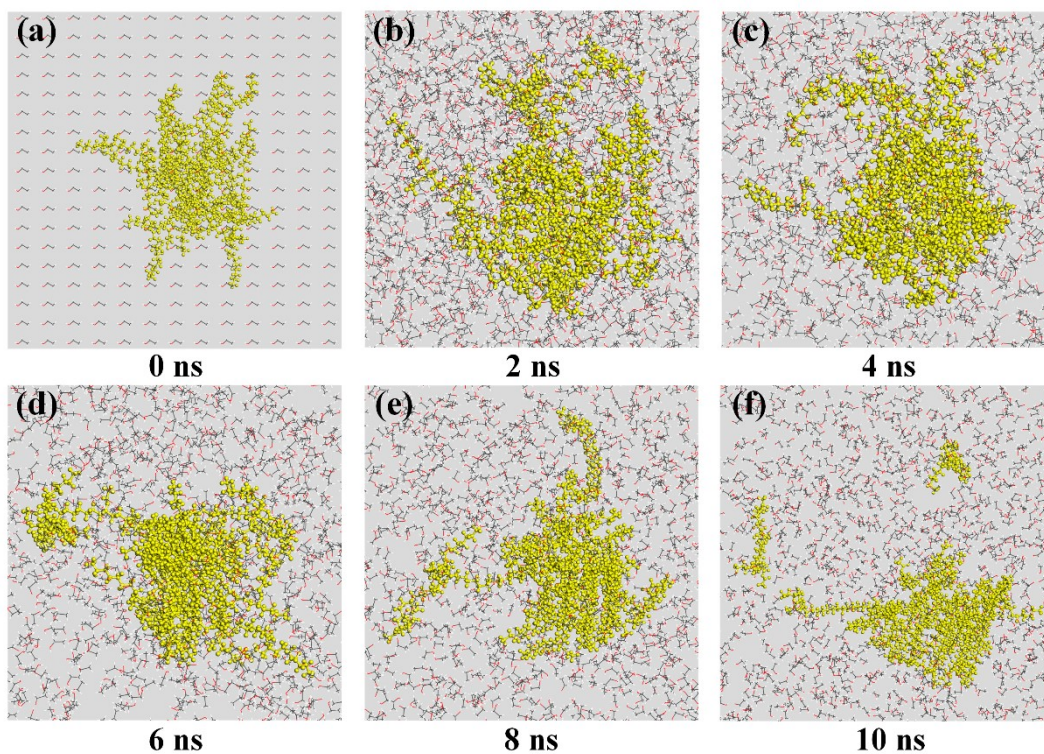


Fig. S4. The aggregation state changes between ethanol molecules and EVA chains within the first 10 ns.

As shown in Fig. S4, Ethanol molecules also aggregate towards the EVA polymers, and tightly wrap them in the first 2 ns. Similarly, a small part of ethanol molecules also enters the gaps of the EVA aggregate. As the simulation progresses, although a small number of EVA chains showing a tendency to gradually separate away, the overall EVA aggregate continues to maintain a closely compacted state.

S5. The aggregation state changes between water molecules and EVA chains.

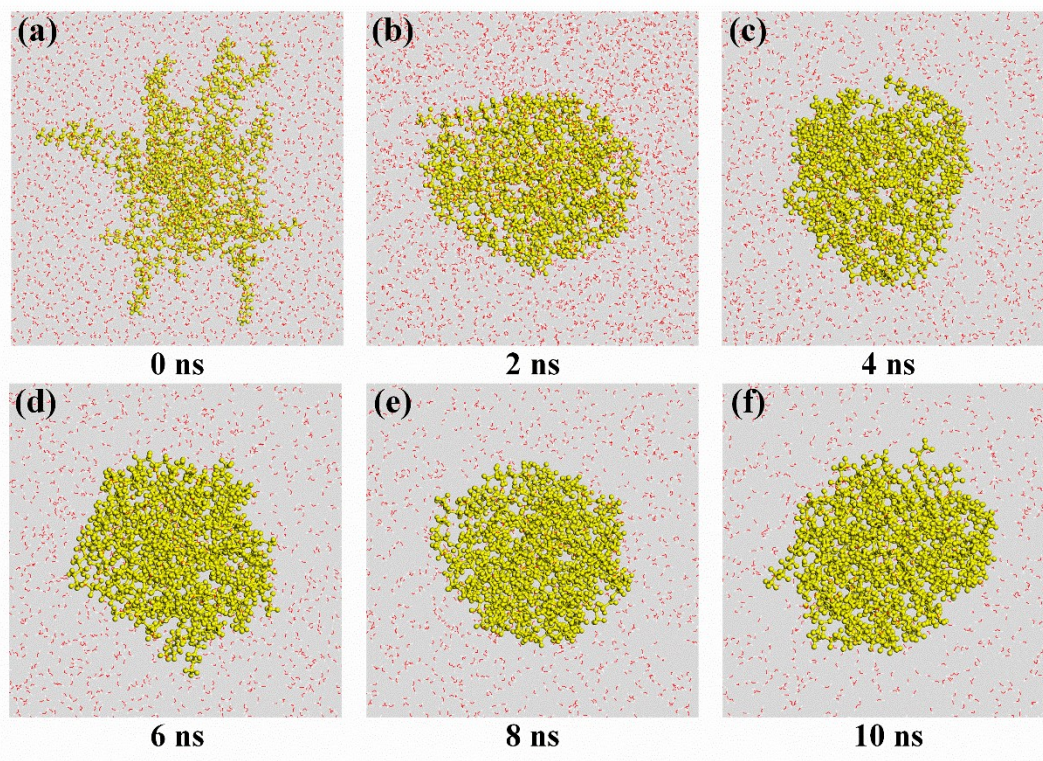


Fig. S5. The aggregation state changes between water molecules and EVA chains within the first 10 ns.

As shown in Fig. S5, in contrast to d-limonene and ethanol, water molecules exhibit no aggregation trend towards the EVA polymers throughout the first 10 ns of the simulation. Instead of penetrating the interior of the EVA aggregate, they just gradually spread outward and away from the aggregate. Moreover, the EVA chains in water aggregate even more tightly.

S6. The number of solvent atoms within a 0.5 nm radius around the EVA chains.

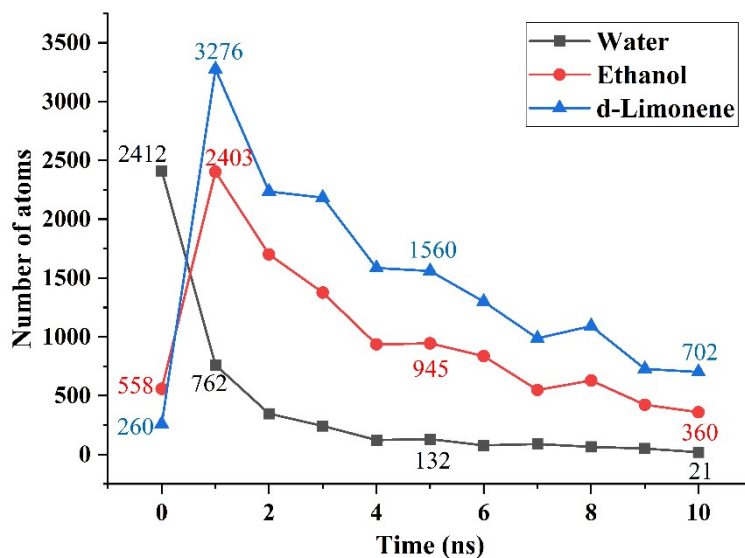


Fig. S6. The number of solvent atoms within a 0.5 nm radius around the EVA chains.

Considering the differences in the total number of solvent molecules, the PSM was defined as the ratio of the number of solvent molecules within a 0.5 nm radius around the EVA chains to the total number of solvent molecules. In Materials Studio, the specific method was to consider each EVA chain as a reference, calculate the number of solvent atoms within a 0.5 nm radius around, and then estimate solvent molecules quantity. As shown in Fig. S6, after the simulation starts, the number of atoms of d-limonene and ethanol around the EVA chains increases rapidly, indicating the aggregation of these two solvent molecules toward the EVA chains. Conversely, the number of water atoms decreases rapidly, reflecting the distancing of water molecules from the EVA chains.

S7. The radius of gyration (RG) data of the EVA aggregate in the three solvents.

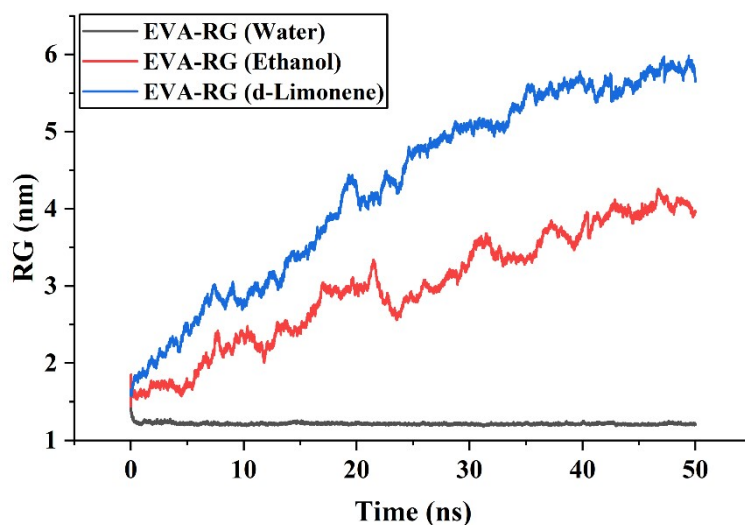


Fig. S7. The radius of gyration (RG) data of the EVA aggregate in the three solvents.

Fig. S7 shows the changes in the radius of gyration (RG) data of the whole EVA aggregate in the three solvents over time. In d-limonene and ethanol, the RG values of EVA aggregate gradually increase during the simulation process, slow down after 40 ns, and finally stabilize at around 6 nm and 4 nm, respectively. The RG of EVA aggregate in water always remain within 1.5 nm. This indicates that in d-limonene and ethanol, the diffusion of some EVA chains causes the overall spatial scale of the aggregate to gradually increase, while in water, the chains remain their aggregation state, keeping the scale nearly unchanged.

S8. The polymer-polymer interaction energy data.

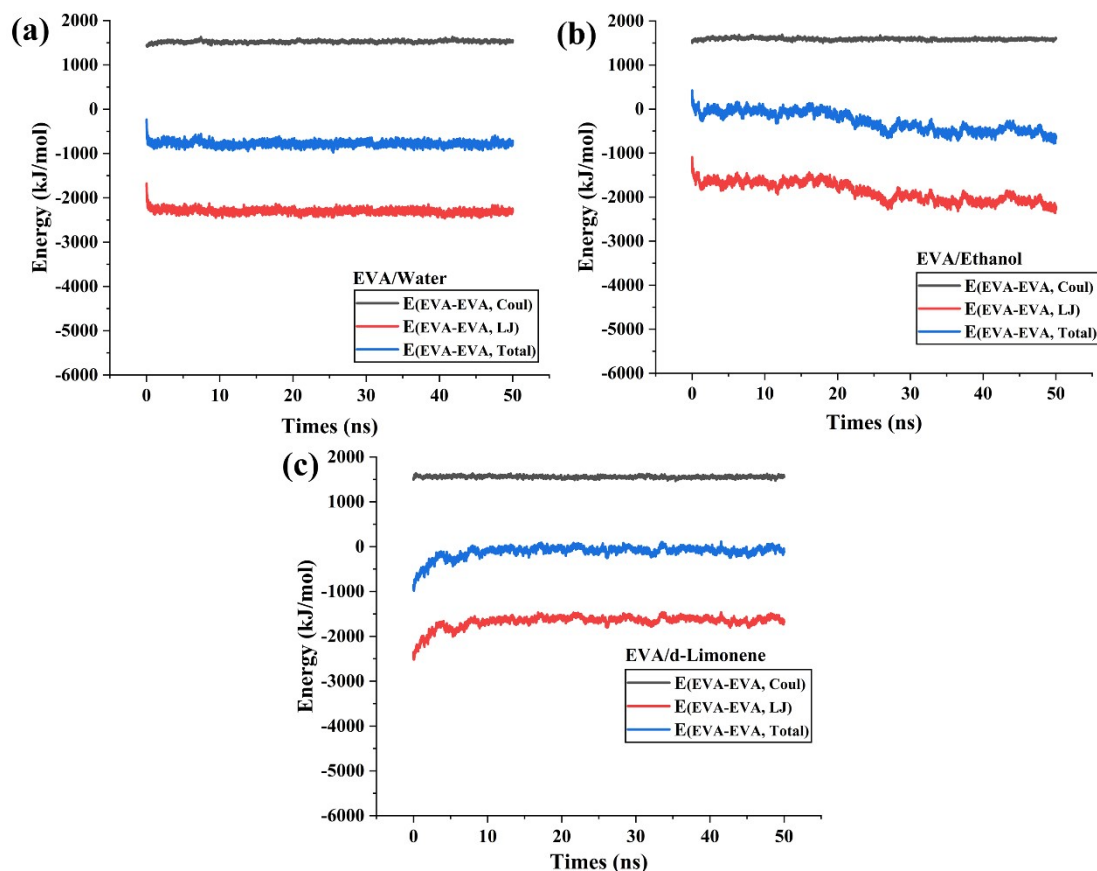


Fig. S8. The polymer-polymer interaction energy data in water (a), ethanol (b), and d-limonene (c).

In the gmx energy calculations, total energy data for polymer-polymer interactions in the three systems are obtained. Fig. S8 shows that the average Coulomb interaction energies between EVA components in the three systems are similar, which are 1525.09 kJ/mol (in water), 1590.36 kJ/mol (in ethanol), and 1556.62 kJ/mol (in d-limonene), respectively. While the average VDW interaction energies are -2300.20 kJ/mol, -1877.28 kJ/mol, and -1669.57 kJ/mol, resulting in total energy averages of -775.11 kJ/mol, -286.92 kJ/mol, and -112.95 kJ/mol, respectively. It can be seen that in water, ethanol, and d-limonene, the interaction energies between EVA components are negative, showing attractive effects.

S9. The solvent-solvent interaction energy data.

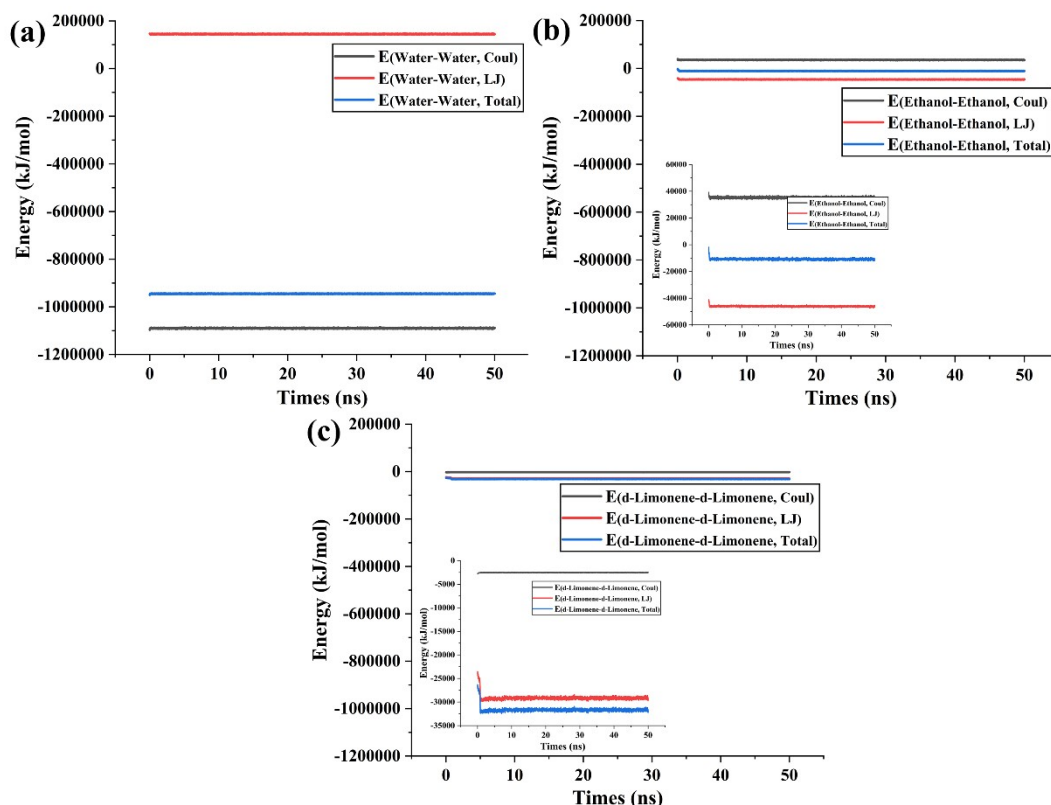


Fig. S9. The solvent-solvent interaction energy data of water (a), ethanol (b), and d-limonene (c).

In the gmx energy calculations, total energy data for solvent-solvent interactions in the three systems are obtained. As shown in Fig. S9, the total interaction energies between solvent components are relatively high in all three systems due to the large number of solvent molecules. Among them, the strong Coulombic interactions between water components result in a total interaction energy of -945,018.18 kJ/mol, while the total interaction energies for ethanol and d-limonene components are -10,802.67 kJ/mol and -31,629.36 kJ/mol, respectively.

S10. The VDW interaction energies of each EVA chains in water solvent.

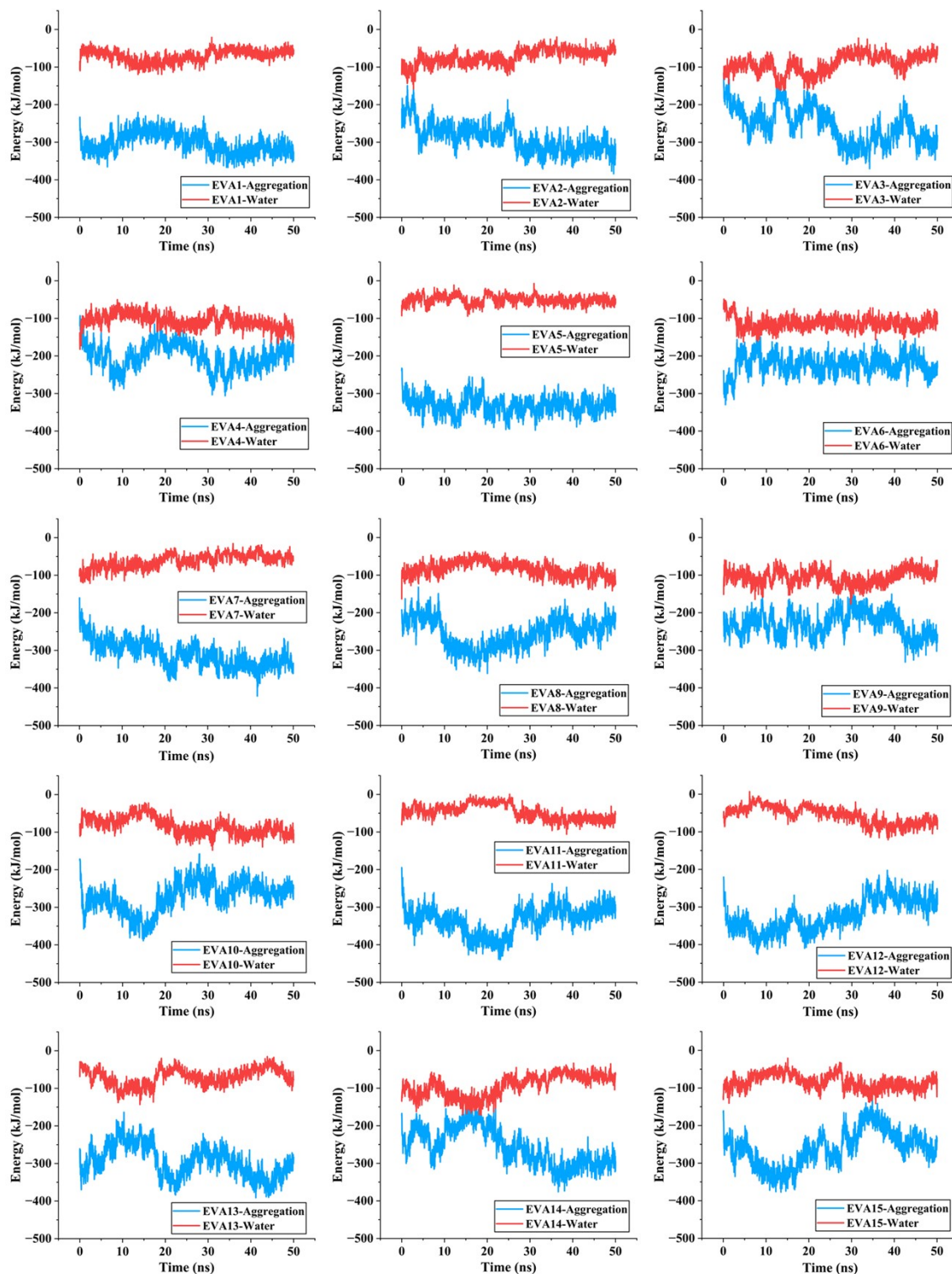


Fig. S10. The VDW interaction energies of each EVA chain in water solvent.

As shown in Fig. S10, for each EVA chain in water, the VDW interaction energy from water molecules is obviously lower compared to that from the other EVA chains

within the aggregate, with an average difference of 196.62 kJ/mol. This difference in the interaction intensity indicates that the mutual attractive forces between EVA chains are stronger than the attractions of water molecules to EVA chains. Therefore, the EVA chains remain closely aggregated, without undergoing separation.

S11. The VDW interaction energies of each EVA chains in d-limonene solvent.

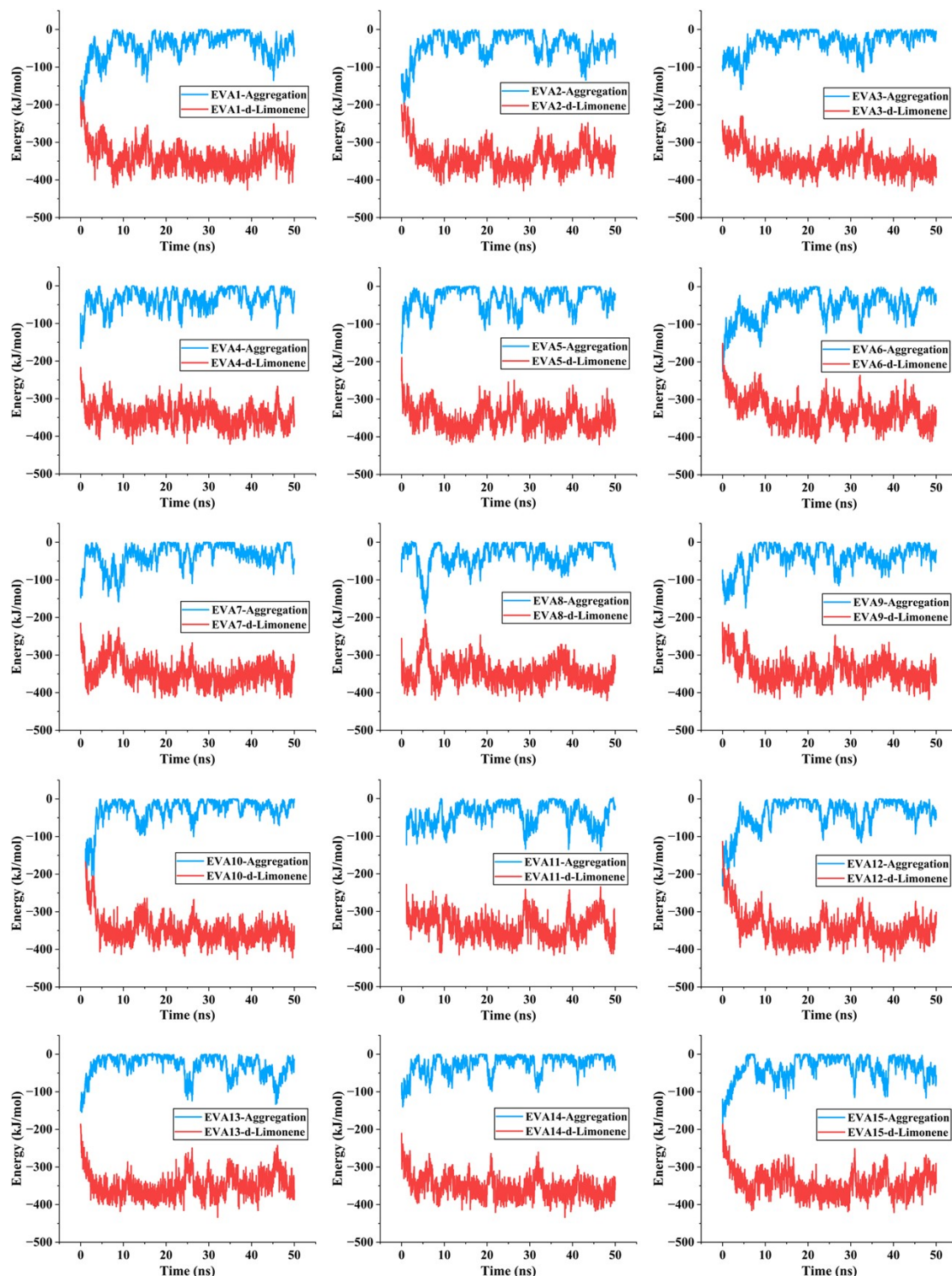


Fig. S11. The VDW interaction energies of each EVA chain in d-limonene solvent.

As shown in Fig. S11, in d-limonene, the VDW interaction energy between each EVA chain and d-limonene molecules is significantly stronger than that with the other

EVA chains within the aggregate, leading to an average disparity of 308.09 kJ/mol. This notable disparity suggests a pronounced attraction of d-limonene molecules to individual EVA chains, surpassing the intermolecular attractions among the EVA chains. Consequently, a gradual swelling occurs in the EVA polymer.

S12. The VDW interaction energies of each EVA chains in ethanol solvent.

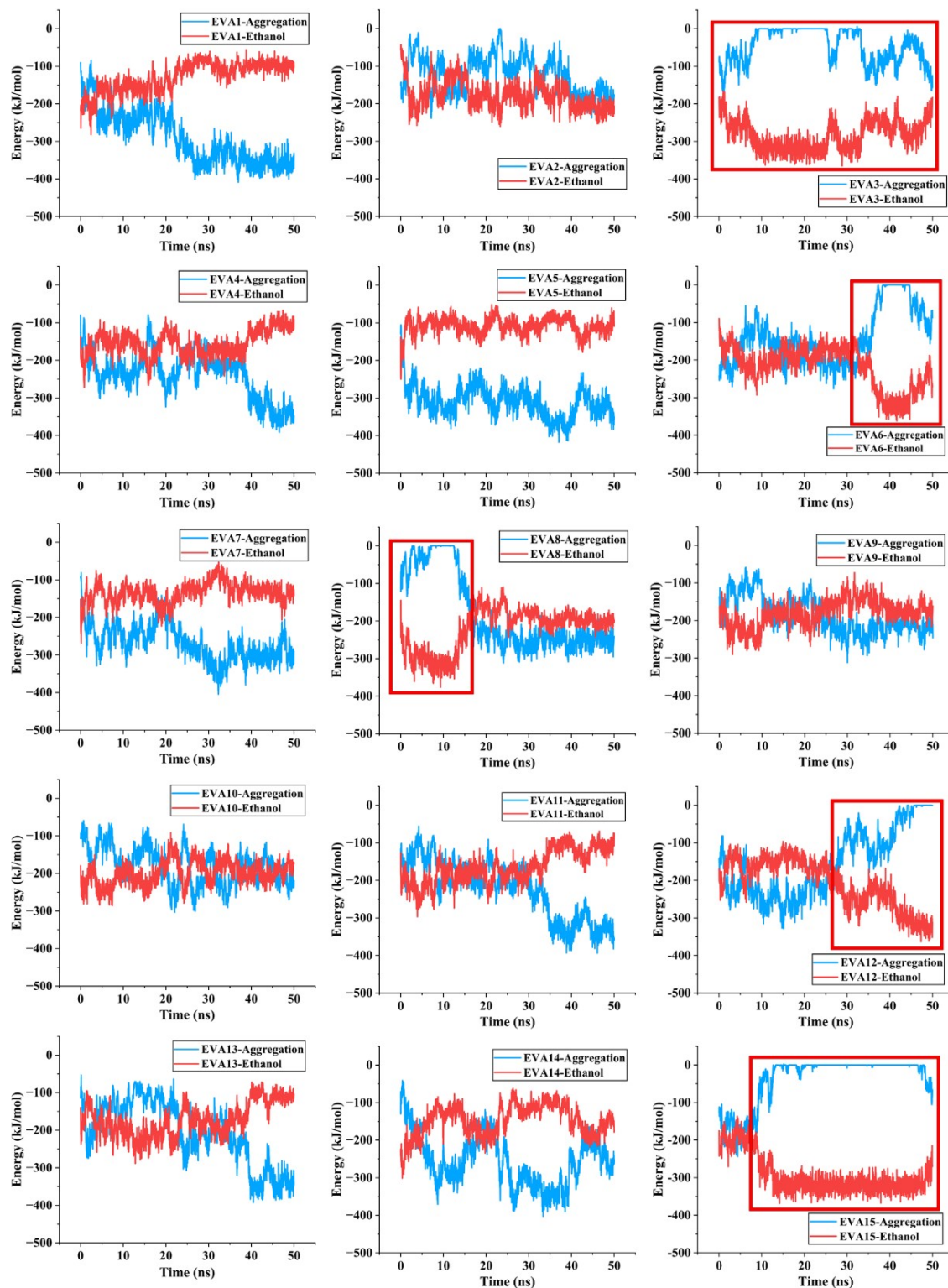


Fig. S12. The VDW interaction energies of each EVA chain in ethanol solvent.

Different from the water and d-limonene systems, two types of VDW interaction energy of distinct EVA chains experience noticeable discrepancies in ethanol solvent

as shown in Fig. S12. On average, the EVA chains are subject to close VDW interaction intensity from ethanol molecules with that from the other EVA chains in the aggregate, with an average difference of only 2.04 kJ/mol. However, for the five EVA chains - EVA3, EVA6, EVA8, EVA12, and EVA15, the VDW interaction energies from ethanol molecules are significantly greater during specific time intervals. This implies stronger attractions from the solvent, which make them gradually separate from the EVA aggregate. In contrast, the remaining ten EVA chains experience VDW interaction energies from ethanol molecules that are either lower or close to those from other EVA chains, maintaining their aggregated state.

S13. The solvent accessible surface area (SASA) data of EVA aggregate in the three different solvents.

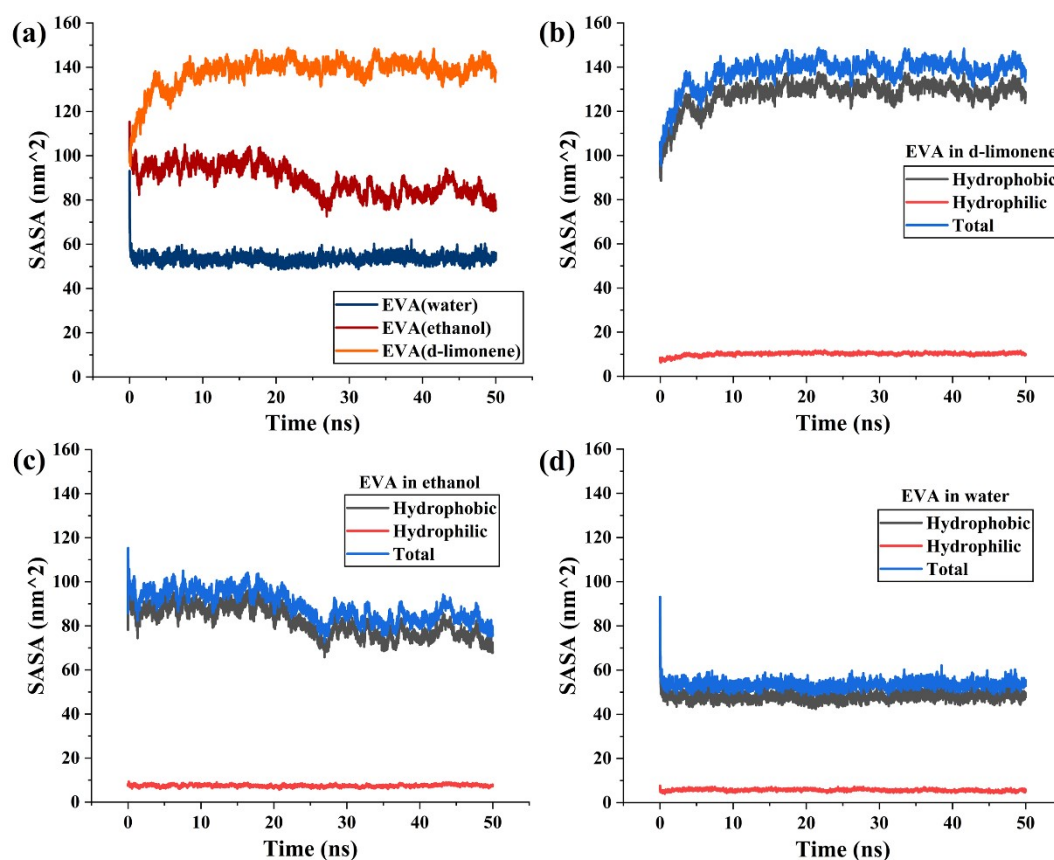


Fig. S13. The SASA data of EVA aggregate in the three different solvents.

The SASA data were calculated with the `gmx sasa` utility using a probe radius of 0.14 nm. As shown in Fig. S12(a), the average SASA values of EVA aggregate in different solvents are 137.95 nm², 88.92 nm², and 53.52 nm², corresponding to d-limonene, ethanol, and water systems, respectively. This change is mainly attributed to the difference in swelling behaviors of EVA: in d-limonene, EVA aggregate is highly swollen, the distance between EVA chains increases, and more segments are exposed; while in water, EVA chains are closely spaced aggregation, resulting in a significant reduction in the total solvent accessible surface area. In addition, further decomposition of the SASA data reveals that the hydrophobic surface areas of EVA aggregate in the three solvents are 127.78 nm², 81.45 nm², and 47.85 nm², respectively, while the hydrophilic surface areas are only 10.17 nm², 7.47 nm², and 5.67 nm², respectively (Fig. S12(b), S12(c), and S12(d)). It is evident that the hydrophobic surface area is

significantly larger than the hydrophilic surface area, indicating that the EVA aggregate exhibits strong hydrophobicity.